Journal of the European Ceramic Society 23 (2003) 331–343

www.elsevier.com/locate/jeurceramsoc

# Effect of annealing and chemical strengthening on soda lime glass erosion wear by sand blasting

Chabane Bousbaa, Abderrahim Madjoubi, Mohamed Hamidouche, Nourredine Bouaouadja*

*Laboratory of Non Metallic Materials, Department of Optics, Mechanics, Faculty of Engineering, University Ferhat Abbas, Sétif 19000, Algeria*

Received 8 February 2002; received in revised form 18 May 2002; accepted 1 June 2002

**Abstract**

The purpose of this work is to study the effect of ion exchange strengthening on the erosion wear resistance of a soda lime glass exposed to sand blasting and to examine the influence of the residual stresses introduced during sand blasting. All sand blasting erosion tests were carried out in laboratory at normal incidence with a sand flux velocity of 12 m/s using incremental eroding masses up to a cumulative mass of erodent of 210 g. Three sets of glass samples were used for this study. The first set of glass samples was strengthened by ion exchange in a salt bath containing a mass of 98% $KNO_3$ and 2% $Al_2O_3$. Glass samples of the second set were exposed to sand blasting in their as received state whereas those of the third set were submitted to an annealing treatment after each incremental erosion test in order to eliminate any residual stresses introduced during sand blasting. After a detailed characterization of the sand used and the determination of the mechanical properties (microhardness and fracture toughness) of both the treated and untreated glasses, we compared the evolution of the mass loss, the erosion rate, the roughness and the optical transmission as a function of the eroding mass for the three sets of glass samples. The results show that the ion exchange treatment improves slightly the glass erosion resistance mainly for small eroding sand masses. The ion exchange treatment becomes less effective beyond an erodent mass of 120 g where the erosion rate for the different sets tend toward nearly the same steady state. All the mean arithmetic roughness curves show a maximum in the interval (90–120) g and tend after a slight decrease toward the same value ($Ra \approx 2.2$ μm). The optical transmission decreased sharply for all glasses independently of the treatment they received after a surface degradation with a mass of 210 g. The difference in the behavior of the as received glass samples and of those annealed after each incremental test reveals the importance of the residual stresses introduced during sand blasting. They seem to effectively enhance the mass loss.


*Keywords:* Cracks; Erosion; Glass; Sand blasting; Surface properties

## 1. Introduction

In Saharan regions, glass articles are frequently exposed to sand blasting damage. The glass surfaces are deteriorated by the impact of fine sand particles of different shapes carried by the wind. The material removal caused by these repetitive impacts can be detrimental to the glass mechanical strength and its optical properties.

This kind of solid particle erosion on soda lime glass takes place essentially by brittle fracture. There is a resemblance between the morphology of the cracks caused by sand blasting and those obtained by sharp quasi-static indentation. The impacts of sand particles induce elastic–plastic fractures where lateral cracks are responsible for the material removal. This occurs by chipping when the lateral cracks interact with each other and with the glass surface. Radial cracks traces can also be observed on the glass surface like radial/median cracks obtained by Vickers indentation.

In general, the kind and extension of solid-particle erosion of brittle materials are affected by the properties of the target material (hardness $H_T$, fracture toughness $K_{CT}$), the properties of the erosive particles (hardness $H_P$, fracture toughness $K_{CP}$, shape, size and specific gravity) and by external conditions (impact velocity, incidence angle and temperature) as shown in Fig. 1.[1] Despite the complexity of the erosion of brittle materials due to the

* Corresponding author.
*E-mail address:* cbousbaa@yahoo.fr (Chabane Bousbaa).

0955-2219/02/$ - see front matter 
PII: S0955-2219(02)00169-3

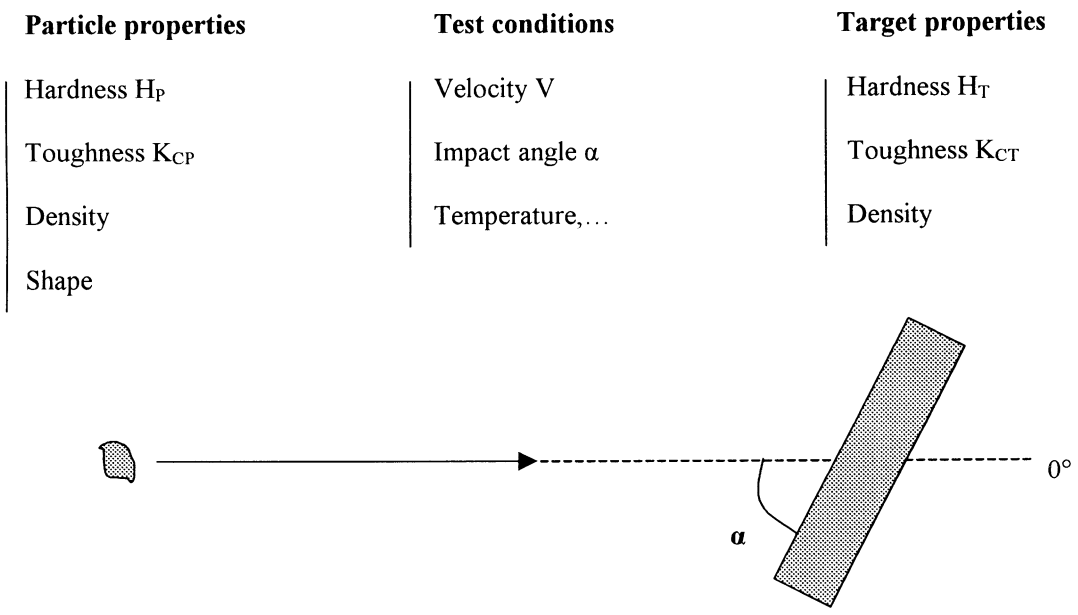


Fig. 1. Parameters to consider in solid particle erosion.

interdependence of these parameters, some advanced theoretical and experimental understanding of the phenomena have been sought in the recent past.[2–21]

Most developed models of the erosion rate during solid-particle erosion of brittle materials were based on the depth and the extent of the lateral cracks using indentation theory. The analysis is made using either quasi-static indentation theory[2–4] or including dynamic effects[5] at normal angle incidence. These models of erosion by elastic-plastic fracture show the importance of the fracture toughness of the target material $K_{CT}$ and to a lesser extend its hardness $H_T$ for improving its erosion resistance. Different relations of these two properties to the erosion rate of brittle materials (ceramics and ceramic composites), developed by Wada and Watanabe[6–8] using multiple regression analysis of experimental data confirm the importance of their effect. The quantity $H_T/K_{CT}$ representing the brittleness of the target material[9] was also used as a guide for erosion resistance.

A Hertzian type of fracture characterised by a purely elastic deformation and the formation of cone cracks can occur when the erosive particles are blunt or softer than the target material.[1] This type of brittle cracking, hardly observed in our experimental work dealing with glass sand blasting erosion, can cause material removal when cone-cracks interact.[10] Different models of this type of brittle erosion were also developed by the past.[10,11]

The lateral cracks nucleate in the plastic zone developed at the impact sites when a critical load of the erosive particles is reached whereas Hertzian cracks initiate their propagation from surface flaws surrounding the impact sites.[12] The critical load for the lateral cracks formation is related to the target mechanical properties (fracture toughness and hardness) and remains independent of the surface condition (prior surface flaw size and density). Contrary to the Hertzian type of erosion, it is not necessary to have a perfectly polished surface to improve the glass erosion resistance caused by elastic-plastic fracture such as sand blasting erosion.

The effects of the particles properties ($K_{CP}$ and $H_P$) on the erosion wear of brittle materials were also considered by some authors.[13–15] A study of the erosive wear of different brittle materials using erosive particles with different hardness[14] shows that target materials having small fracture toughness such as glass are eroded essentially by brittle fracture. When the necessary impact energy is reached, the erosion mechanism is of the Hertzian fracture type with softer erosive particles ($H_P/H_T<1$) or of the elasto-plastic fracture type with harder erosive particles ($H_P/H_T>1$). Another study on the effect of the particles toughness on the erosive wear of brittle materials[15] shows the tendency for an increase of the erosion rate with tougher particles at an impact angle of 80° and no clear relation when the impact angle is 30°. The authors explained this difference in the effect of the particles fracture toughness by the different erosion mechanisms encountered with the two impact angles. The erosion is characterised essentially by brittle fracture with a 80° angle and scratching with a 30° angle.

Studies on the effect of the incidence angle on the erosion rate on brittle materials show that the maximum erosion is reached at normal incidence. This is also the case for glass sand blasting erosion as was shown in a previous work.[16] On ductile materials, the material removal is obtained by plastic deformation and reaches its maximum rate at shallow impact angles (around 30°

impact angle). However, It was also shown that even glass tends to be eroded by plastic deformation similarly to ductile materials when eroded by very fine particles or at low velocities.[1] One particular study shows indeed that the erosion rate of a soda lime glass eroded by 9 μm silicon carbide particles at a velocity of 136 m/s reaches its maximum at around a 30° incidence angle.[17]

The "ductile" type of erosion on brittle materials is characterised by minor chipping with no crack formation. According to I.M. Hutchings,[1] the transition in the erosion mechanism from plastic deformation to brittle fracture was explained by the necessary collision energy of the particle to reach a certain threshold. He proposes for different engineering materials that the dimensionless expression ($K_{CT}^2/r.H_T^2$), where $r$ is the radius of the particle, can be used to determine the nature of the dominant erosion mechanism. Lower values of this expression would indicate the presence of brittle fracture.

To describe the nature and the mechanism of erosion of different materials, other authors[18] proposed instead a new parameter known as the erosion efficiency $\eta$ defined as:

$$\eta = 2.\mathrm{Er}.H/\rho.V^2 \quad (1)$$

where Er is the erosion rate, $H$ the hardness, $\rho$ the density of the target material and $V$ the velocity at impact.

This efficiency can reach 1000% in the case of glasses which behave in an ideally brittle manner in erosion tests.

Besides, theoretical erosion maps based on the onset of fracture in the elastic and plastic regime were derived to show the erosion mechanism transitions.[19,20]

It is also interesting to note that repeated quasi-static Vickers indentations on soda lime glass with subthreshold loads was shown to lead to an increase of the plastic zone until radial cracks appear after a certain number of cycles.[21] The cracking starts when the residual stresses produced by these cumulative impressions become critical. Comparatively, we could study the effect of the residual stresses induced during solid particle erosion with repetitive fine particles impacts as is the case with glass sand blasting at different velocities.

The usual way used for reducing impact damage on glass is to put its surface in compression. This can be achieved by thermal tempering, ion-exchange, vitreous enamelling or by cladding with a material of lower thermal expansion.[22] The thermal tempering or cladding methods give a relatively thick compressive surface layer in comparison with the two other methods. It was shown that the compressive surface stress field produced by thermal glass tempering does not improve significantly the glass erosion resistance to sharp particles[23] as was noticed in sand blasting or by Vickers indentation, but it could certainly improve the material erosion resistance caused by Hertzian cracking. The extent of the lateral cracks produced by Vickers indentation can be more pronounced if the glass is thermally tempered.[24] Other studies have shown that glass tempering can have a small effect on its hardness and its elasticity modulus by reducing them while the fracture toughness seems to remain unchanged.[25,26] This effect is due to the more open structure of the glass obtained by rapid cooling.

Ion-exchange is a chemical treatment which consists of exchanging small ions by larger ions in the glass surface using a molten salt bath. The expansion of the glass structure generates a compression at the surface and a balancing tension in the interior. This treatment is simple but costly when used industrially. According to I.W. Donald,[27] the thickness of the compressive layer varies from a few micrometers up to several hundreds micrometers in dependence of the glass composition, the treatment conditions and the sample thickness. Among the main advantages of this treatment is that we can obtain higher mechanical strengths and avoid glass distorsion since it is usually made at a temperature lower than the transition point. To our knowledge, the effects of structural changes obtained by chemical strengthening or by coating techniques on the mechanical properties ($K_{IC}$, Hv, $E$) and thus on the glass erosion resistance, are not completely established.[28–32]

Our goal in this work is to study the effect of annealing and chemical strengthening on a soda lime glass erosion when exposed to sand blasting. We have projected variable incremental erodent masses up to 210 grams normally to samples at a flux velocity of 12 m/s. The samples were differently treated: as received, annealed and chemically strengthened. We have determined the evolution of mass loss, erosion rate, roughness and optical transmission as a function of the incremental eroding sand mass.

## 2. Experimental procedure

### 2.1. Material characteristics

#### 2.1.1. Glass characteristics and samples preparation

The material used in this study is an ordinary soda-lime-silica glass which was delivered in its as received state with a 3 mm thickness. Its mean chemical composition and some of its physical characteristics are given in Tables 1 and 2.

The microhardness and the fracture toughness of the as received and annealed glasses were measured by

Table 1
Mean chemical composition of the glass used

| Oxides | $SiO_2$ | CaO | $Na_2O$ | MgO | $Al_2O_3$ | $Fe_2O_3$ | Others |
|---|---|---|---|---|---|---|---|
| Mass (%) | 71.56 | 7.92 | 13.73 | 4.21 | 1.32 | 0.097 | 1.163 |

Table 2
Some of the physical glass properties

| Properties | Values |
|---|---|
| Thermal dilatation coefficient $\alpha$ | 8.5 $10^{-6}$ $K^{-1}$ |
| Young modulus $E$ | 72 GPa |
| Poisson's coefficient $\nu$ | 0.22 |
| Density $\rho$ | 2.47 g/cm$^3$ |
| Transition temperature $T_g$ | 530 °C |

Vickers indentation using a load of 1 N and a dwell time of 20 s. We could not use a load less than 1 N for the hardness measurements in order to reach the depth of the roughness valley of the eroded glass. The dimensional measurements of the imprint diagonals and of the radial micro-cracks were made on an optical microscope (Neophot 21). For the indentation tests made on the chemically treated glass, loads within the interval (0.6–0.8) N were under the threshold necessary for the initiation of radial cracks while loads above 1 N induce sometimes rapid chips formation impeding the radial cracks observation. As the ratio $l/a$ (with $l = c - a$) of the radial crack on half the diagonal is smaller than 2.5 for the loads used, we supposed that we have a Palmqvist type of crack system and choose the following Niihara's model[33] for obtaining the fracture toughness.

$$K_{1c} = \frac{0.035}{\phi}\left(H.a^{1/2}\right)(E.\phi/H)^{0.4}(l/a)^{-0.5} \quad (2)$$

where $H$ is Vickers hardness, $E$ the Young's modulus and $\phi$ a factor representing the ratio $(H/\sigma_y)$ taken approximately equal to 3.

In Table 3, are given the values of the glasses hardness $Hv_T$, fracture toughness $K_{CT}$ and also the mean imprint depths.

We prepared from the same soda-lime glass sheet, glass samples having the same dimensions $50\times50\times3$ mm$^3$ in three different states:

- The first samples set was prepared in their as received state without any treatment.
- The second set was annealed before and after each incremental erosion test in order to eliminate any preliminary residual stresses or those induced during each incremental erosion test. The annealing treatment was made at a temperature of 510 °C during one hour with a heating temperature rate of 3 °C/min and a cooling temperature rate of 2 °C/min.
- The remaining glass samples were strengthened by ion exchange making the glass surface in compressive state. The chemical treatment was made in a salt bath containing a mass of 98% of $KNO_3$ and 2% of $Al_2O_3$ at a temperature of 480 °C during 5 h.

Table 3
Hardness, fracture toughness and mean imprint depth for the three types of glass

| Glass state | As received | Annealed | Chemically tempered |
|---|---|---|---|
| $Hv_T$ (GPa) | 5.78±0.13 | 5.91±0.25 | 6.61±0.20 |
| $K_{CT}$ (MPa$\sqrt{m}$)[33] | 0.84±0.021 | 0.78±0.018 | 1.85±0.085 |
| Mean imprint depth (μm) | 3.62 | 3.58 | 3.38 |

### 2.1.2. Sand characteristics

The sand chosen for this study comes from the region of Ouargla in the Saharian region sited at the oriental Erg in Algeria. It was used in its as received state without any preliminary washing. Fig. 2 represents a sand sample showing the particles shape and average size. We noticed that the sand is composed from differently shaped and colored particles. Some of these particles are limpid and translucent. The sand particles granulometry distribution for a sand mass of 100 g is not very dispersed (Fig. 3). It was obtained using a series of sieves. With successive sieving periods of 15 minutes, the distribution expressed in a histogram form (Fig. 4) shows that most sizes lay in the interval (200–250) μm.

The particles appear mostly rounded in shape although sometimes angular forms appear. The roundness is predominant as the elongation index (Ei) measured on a representative sand particles sample shows. This index is defined as the ratio $(Ei = L_p/l_p)$ of the greatest length dimension $L_p$ observed on the sand particle over the greatest dimension $l_p$ measured perpendicularly to $L_p$ (Fig. 2). To determine the grains elongation index, we used a sample of 100 sand particles in the main interval (200–250) μm. We observed that about 20% of theses particles are rounded as the elongation index approached 1 and 70% present a limited

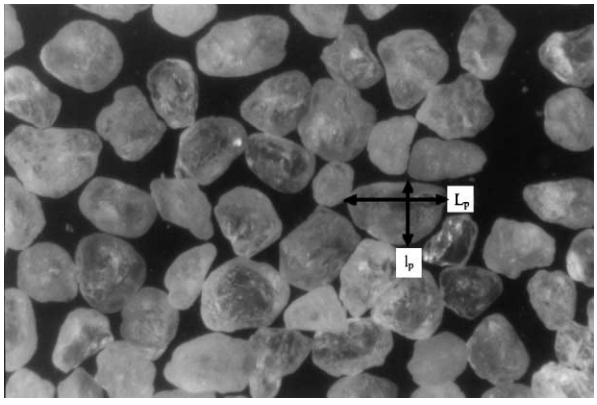


Fig. 2. Micrograph showing the sand morphology and size, and the lengths $L_P$ and $l_P$ to consider in the elongation index determination.

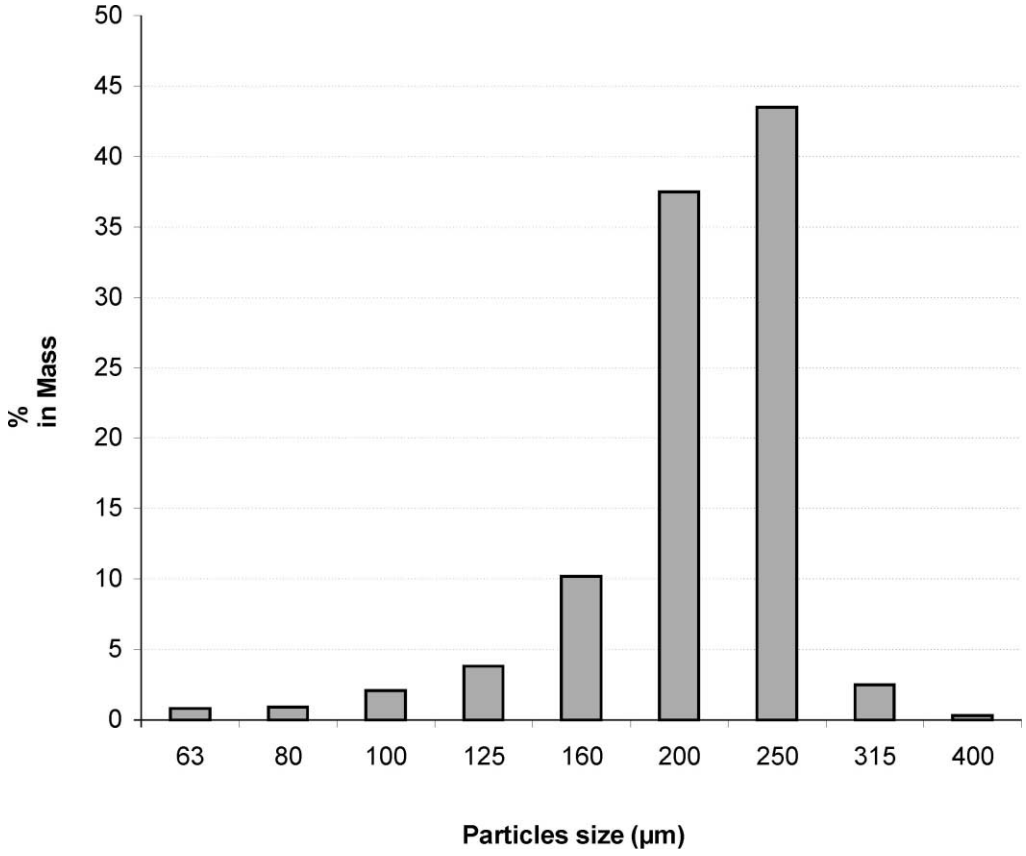


Fig. 3. Granulometry distribution obtained for the sand used.

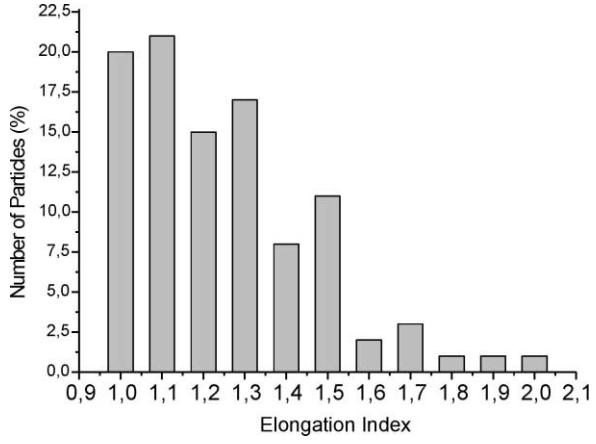


Fig. 4. Histogram showing the elongation index of the sand particles used for a sample of 100 sand particles.

elongation with an index located between 1.1 and 1.5 (Fig. 4).

Colored aspect of the grains suggests they have a diversified mineralogical composition. The principal minerals composing the sand of Ouargla region are brown tourmaline, limetine, limonite, colored quartz and gypsum. The hardness according to Mohs scale of these mineral constituents is given in Table 4.

In order to measure the hardness and the fracture toughness of the sand particles, we glued the particles into a thermosetting resin pellet. Before making the indentations for these measurements, we proceeded to successive micro-grinding operations made with different fractions of alumina oxide (F80, F28 and F10). A polishing final operation, using iron oxide particles of 1 μm mean size, was used to obtain a good flatness of the pellet surface with a well prepared particles surface. We determined the sand particles hardness using a load of 0.6 N and a dwell time of 15 s on a sample of 30 grains. The obtained values present a certain dispersion ($Hv = 14.49 \pm 3.28$ GPa). These values are higher than the glass hardness values despite their diversified mineralogical composition. We attempted to determine the particles fracture toughness with a load of 1 N. Among 30 trials carried out, we notice that radial cracks appear in all cases ($2c = 20.9 \pm 1.8$ μm) and that only one particle disintegrated. Because of the impossibility to measure directly the sand particles Young's modulus, we could not have an estimation of the fracture toughness.

Table 4
Sand mineralogical composition

| Minerals | Quartz | Tourmaline | Limenite | Limonite | Gypsum |
|---|---|---|---|---|---|
| Mohs hardness | 7 | 7–7.5 | 5–6 | 2–5 | 2 |

The sand density ($\rho = 2.639$ g/cm$^3$) was measured on a finely crushed sand sample using a helium pycnometer.

### 2.2. Sand jet impingement apparatus

Different erosion test rigs were proposed in the literature. These depend on the impact velocities used. As recommended by the standards for airborne particles erosion testing (DIN 50 332[34] and ASTM G76 89[35]), we opted for a horizontal jet impingement system. It is composed of an ejector in form of an elongated cylindrical with a conical convergent end allowing regular particle suction. The convergent end of the ejector is tied to a cylindrical nozzle of reduced section and having a length between 1 and 1.5 m enabling the particles to reach nearly the velocity of the air flux carrying these particles. In general, the ratio of the conduit length to its interior diameter $L/\varphi$ has to be in the interval 25–80 in order to avoid turbulent flow and reach a steady flow. In Table 5, we compare our ratio corresponding to 40 with those of other erosion test rigs used and found in literature.[36–42] The greatest ratio found among these that we can notice is 333. The ASTM G76–89 recommends a ratio ($L/\varphi = 25$) while the norm DIN 50 332 proposes a conduct with a length of 120 mm and a diameter of 8 or 18 mm. In this work, the nozzle inner diameter is 25 mm. The inner surface of the conduit is supposed to not influence the velocity profile, as it discussed to by R.J.K. Wood.[42]

### 2.3. Test conditions

The air speed used for projecting the sand particles out of the convergent end was fixed at 12 m/s. All glass samples were placed normal to the sand flux. The distance between the convergent end and the samples is fixed constant to 50 mm for all the erosion tests. The sand mass rate is about 10 g/min and the sand flux is estimated to be 0.338 kg/m$^2$/s. The variable parameter is the cumulative erodent mass: 5, 10, 20, 30, 60, 90, 120, 150, 180, 210 g. During erosion tests, the temperature and humidity rate in the laboratory were nearly constants: $25 \pm 1$ °C and $43 \pm 5$% RH. The mass loss of the samples was measured before and after each experiment on a Sartorius analytical balance with an occuracy of 0.1 mg.

Table 5
Characteristics of some examples of erosion test rigs rates used in literature

| Nozzle conduit diameter $\varphi$ (mm) | Nozzle conduit length $L$ (mm) | Ratio $L/\varphi$ | Velocity (m/s) | References |
|---|---|---|---|---|
| 4.95 | 305 | 62 | 90 | [36] |
| 3 | 90 | 30 | 15–35 | [37] |
| 4.72 | 308 | 65 | 52 | [38] |
| 8 | 100 | 12.5 | 368–423 | [39] |
| 6 | 2000 | 333 | 18–45 | [40] |
| 10 | 3000 | 300 | 300 | [8] |
| 1.5 | 16 | 10.66 | 20–300 | [41] |
| 30 | 2.2 | 13.63 | 10–200 | [20] |
| 16 | 1000 | 62.5 | 300 | [42] |
| 25 | 1000 | 40 | 12 | Present work |

## 3. Results and discussion

### 3.1. Mass loss

Fig. 5 presents the cumulative mass loss evolution as a function of the incremental eroding sand mass for the three glass states. We can observe the same tendency for the three distinct curves. We have a smooth increase of the cumulative mass loss in the beginning up to 60 g of eroding mass and a clear more important augmentation beyond. The curve for the as received glass above that of the annealed glass shows the effect of the residual stresses left by the erosion damage. This effect seems to continuously increase with the mass projected as we can see from the increasing separation of the two curves although the same annealing treatment was taken after each incremental erosion test and the same lapse of time (24 h) was chosen between two successive tests. We cannot speculate at the moment on the effect of the environment (aging) on the mass loss when dealing with such successive erosion tests. This would need further experiments. The effect of the environment on soda lime glass lateral crack formation was approached by Thiruvengadaswamy and Scattergood[43] during indentation cycling tests. They showed that postcycling aging can produce delayed chipping but this remains dependent on the load cycling history. We could have a similar effect with sand blasting.

The chemically strengthened glass curve evolves similarly to but below that of the annealed glass. The difference in the mass loss is more important for small sand masses. It decreases and becomes almost constant beyond a sand mass interval of (90–120) g. The two curves are nearly parallel to each other. The erosion process reaches probably a steady state in all cases after a cumulative sand mass of 120 g, but the chemically strengthened glass remains slightly more resistant to erosion.

The histogram in Fig. 6 shows the evolution of the relative cumulative mass loss for the small incremental eroding sand masses. It seems that we have an incubation period for the strengthened glass corresponding to an eroding mass less than 10 g. The two other glasses (as received and annealed) present some mass loss even with a mass of 5 g.

The following figure shows a general view (Fig. 7A) and some details (Fig. 7B) of the damage generated by

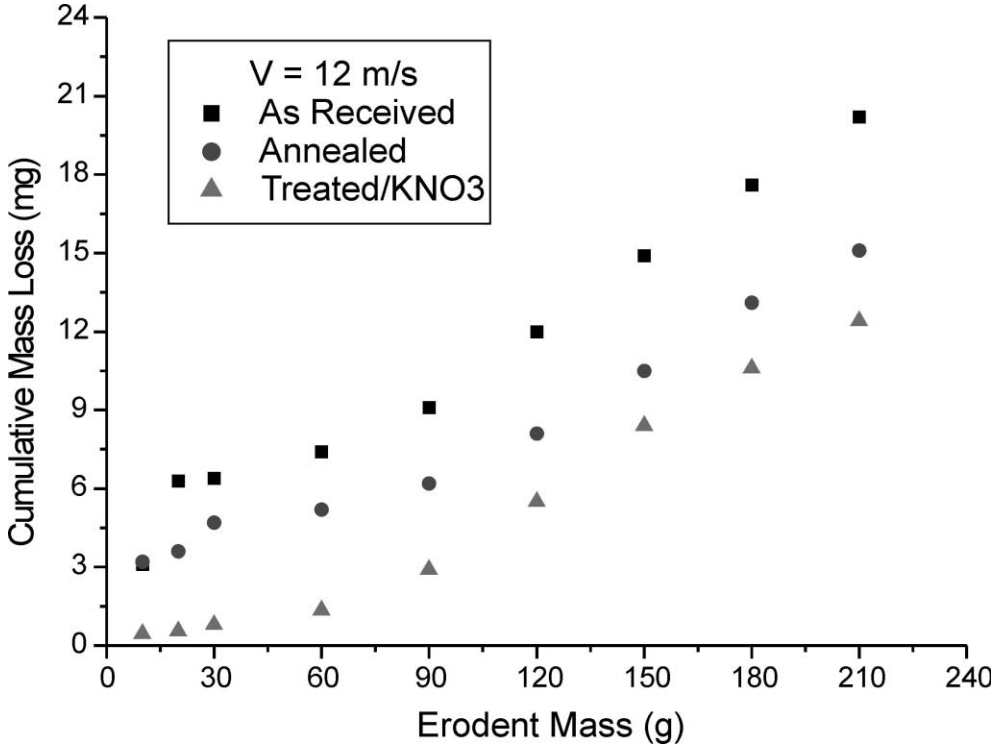


Fig. 5. Cumulative mass loss variation as a function of incremental eroding sand mass.

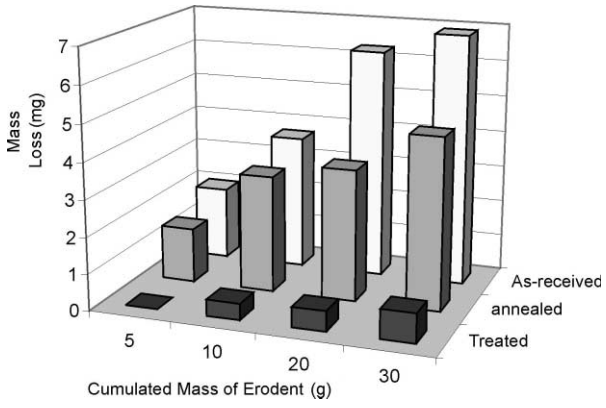


Fig. 6. Histogram showing an incubation period for the strengthened glass in comparison with the as received and annealed samples.

sand blasting on the as received glass. We observe on Fig. 7A that the flaws sizes are variable (singular or multiple) and they are randomly distributed on the eroded surface. The details on Fig. 7B show that the material removal takes place by the formation and propagation of lateral cracks which develop into chippings of different sizes. We can also notice the similarity between the singular impact flaws and the cracks systems obtained by sharp indentation. When there is an interaction between different impact flaws, the erosion mechanisms become complex and therefore difficult to describe.

In Fig. 8 obtained for the strengthened glass, we observe that the flaws induced by sand blasting have a different morphology in comparison with the as received

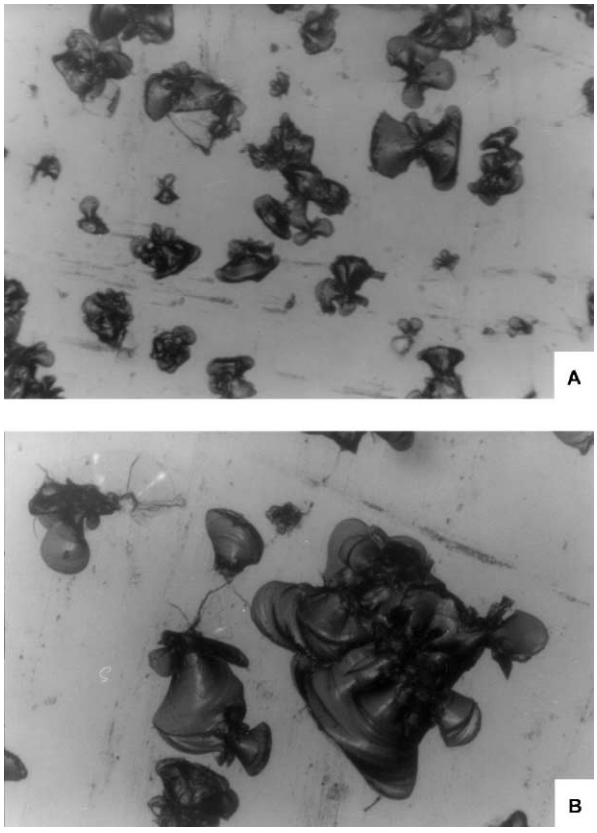


Fig. 7. Micrographs showing a general view (A, ×120) and some details of the flaws generated by sand blasting for the as received glass state (B, ×280).

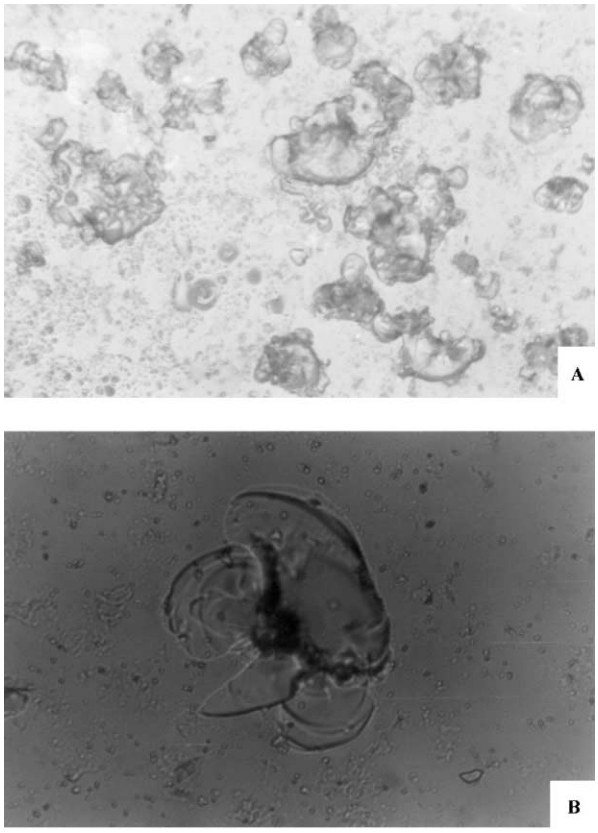


Fig. 8. Micrographs showing a general view of a strengthened glass surface eroded by sand blasting (A, ×120) and some details of an impact morphology (B, ×280).

state (Fig. 8A). The lateral cracks seem to be oriented in all directions inducing a material removal in a closed outline (Fig. 8B). This type of damage configuration is hardly observed in the case of the as received state. In the same test conditions, the singular impact flaws for the strengthened glass seem to have reduced sizes. This is probably related to the improved fracture toughness.

### 3.2. Erosion rate

The erosion rate is determined as the rate of material mass removal against the mass of the particles projected at the sample. Fig. 9 presents the cumulative erosion rate evolution as the eroding mass increases for the different glass states.

The erosion rate of the strengthened glass is clearly smaller than for the two other states especially during the beginning of the erosion process up to a mass of 60 g

Table 6
Hardness ratio, brittleness factor and efficiency obtained for the different glass states in relation with the steady erosion rate

| State | As-received | Annealed | Treated by $KNO_3$ |
|---|---|---|---|
| $Hv_P/Hv_T$ | 2.51 | 2.45 | 2.19 |
| $Hv_T/K_{CT}$ ($m^{-1/2}$) | 6881 | 7577 | 3573 |
| Efficiency $\eta$ (%) | 325.5 | 250.9 | 230.4 |
| Steady erosion rate (mg/g).$10^{-2}$ | 10.1 | 7.55 | 6.02 |

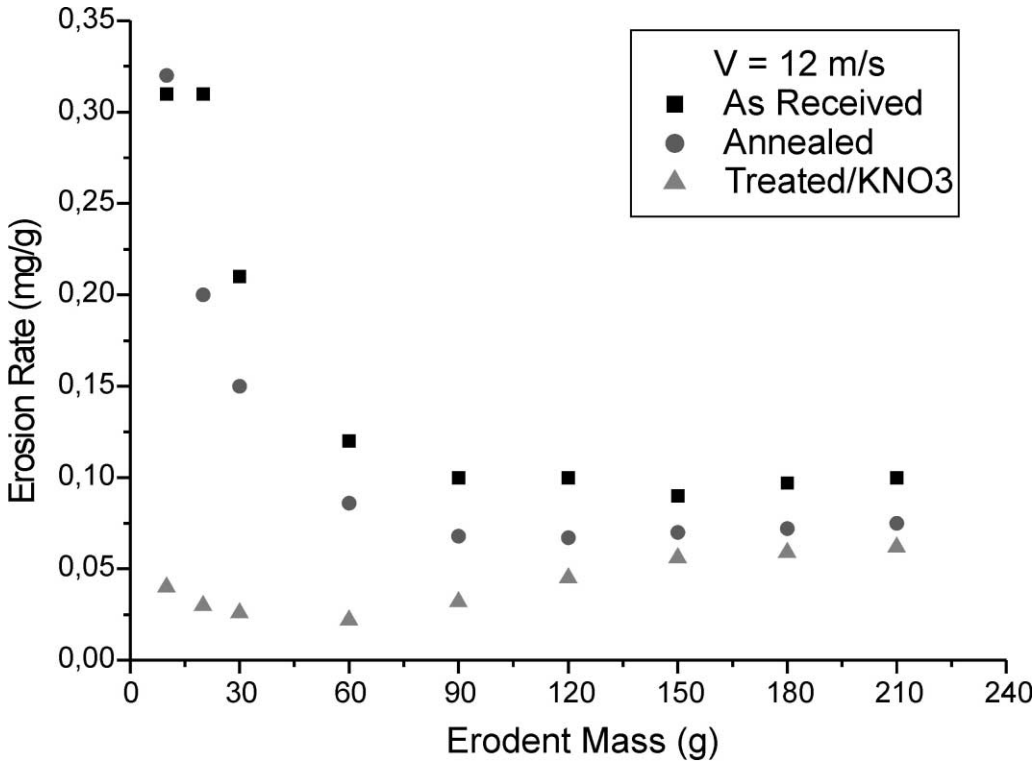


Fig. 9. Erosion rate variation as a function of eroding mass for the three glass states.

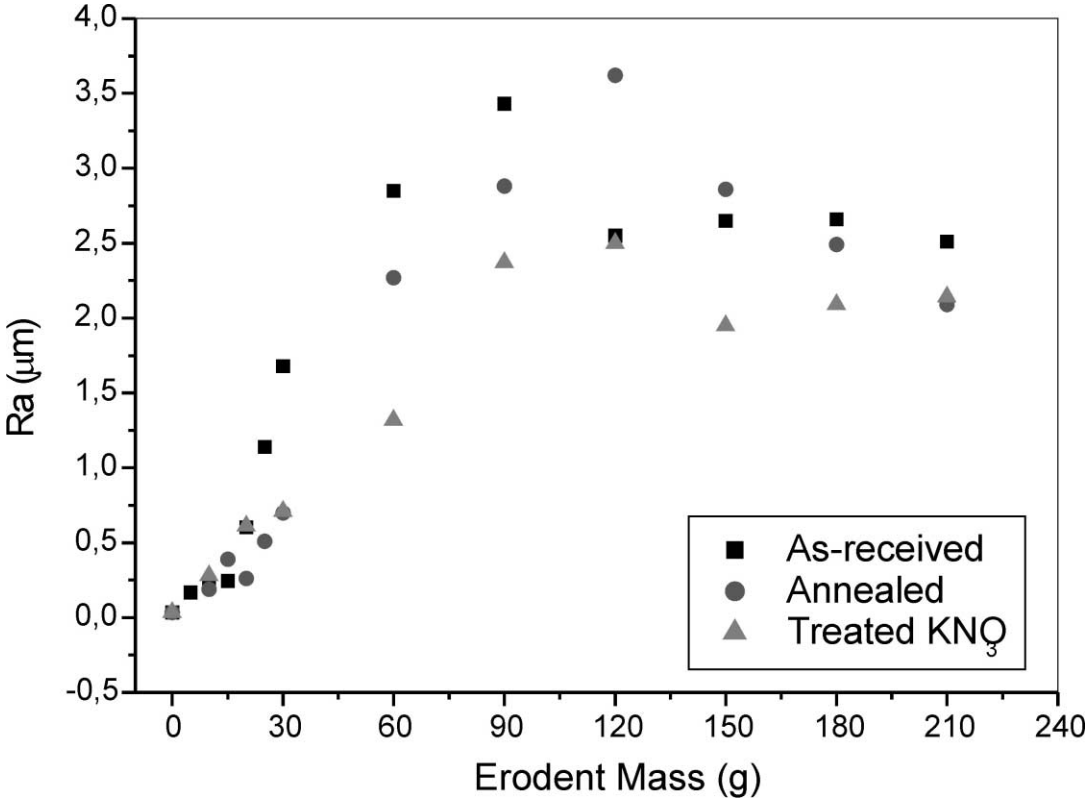


Fig 10. Glass surface roughness as a function of eroding mass for the different states.

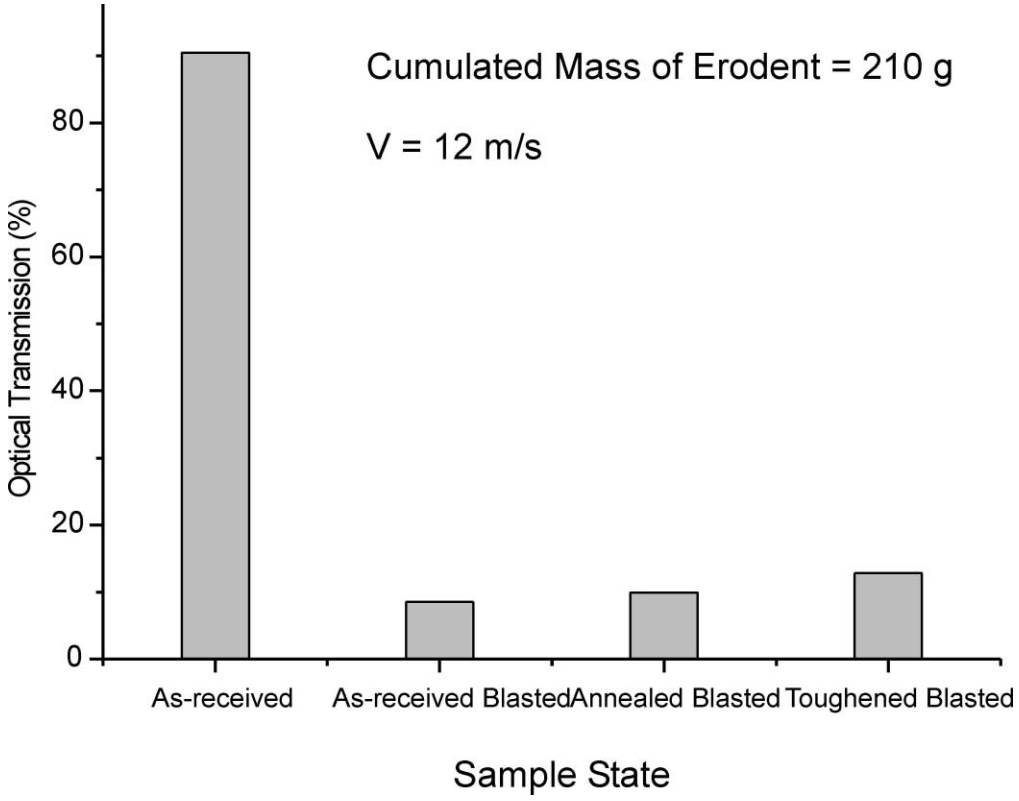


Fig. 11. Mean optical transmission values before and after sand blasting for the different glass states.

of eroding sand. The behaviour of the strengthened glass curve changes also beyond this point in comparison with the other curves. The erosion rate increases before reaching a steady state while the two other curves show a decrease toward nearly the same steady state. The closeness of the curves shows that the chemical treatment used for reinforcing the glass surface against erosion becomes less effective beyond 120 g of eroding mass. According to these results, the chemical treatment used seems to be inefficient for glass erosion resistance during the lasting sandstorms often encountered in Saharian regions.

The effect of the residual stresses induced by the cumulative erosion damage is also apparent in this figure as the curve for the annealed state remains distinctly below that of the as received glass. However the increasing effect of the residual stresses which is apparent in Fig. 9 is less obvious when dealing with erosion rate rather than mass loss. The erosion rate values obtained for 210 g cumulated erodent mass is 10.1, 7.55 and 6.20 $(mg/g)10^{-2}$ respectively for as received, annealed and chemically treated states.

The effect of glass treatment on the hardness ratio ($Hv_P/Hv_T$) and the brittleness index ($Hv_T/K_{CT}$) is shown on Table 6. The steady state erosion rate for each glass state and the efficiency are also indicated. The efficiency values obtained for the three glass samples sets exceed clearly the limit of 100% mentioned by

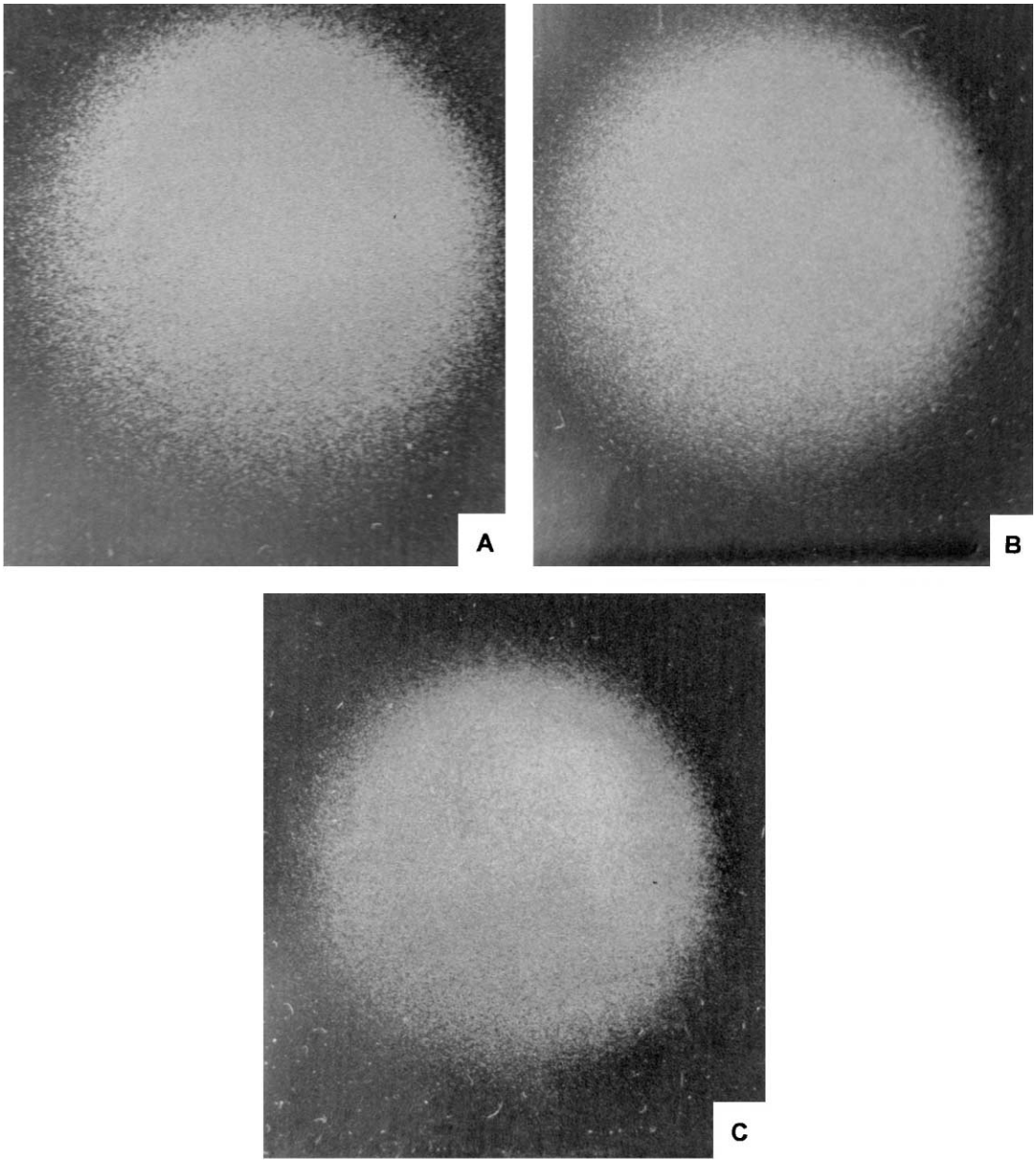


Fig. 12. Micrographs showing the contrast of the eroded zones for the three glass states: (A) as received, (B) annealed, (C) chemically treated.

Manish Roy.[18] These values correspond therefore to a brittle erosion mechanism although the air flux velocity used in our experiments was relatively weak ($V = 12$ m/s).

For a cumulative sand mass of 210 g, the dispersion of the steady state erosion rate for the three glass states is limited to 6–$10.10^{-2}$ mg/g. The strengthened glass has, however, the lowest erosion rate when the corresponding parameters ($Hv_P/Hv_T$ and $Hv_T/K_{CT}$) are the lowest. There is no significant difference of these parameters values for the as received and annealed glasses.

### 3.3. Roughness

The surface roughness was measured in the central zone affected by erosion in the median direction. Fig. 10 shows the surface roughness Ra variation as a function of the sand mass projected for the three glass states. The surface roughness of the non eroded samples is about $Ra = 0.071$ μm. We notice from this figure that the roughness values which are closer for the different glasses at the start, become distinguishable beyond a mass of 20 g of sand mass. They remain smaller when the glass is chemically treated. All the three roughness curves have a maximum followed by a smooth decrease toward a stabilised state. A maximum of 3.43 μm is reached after 90 g of eroding mass for the as received glass. The annealed and treated glasses present a maximum of 3.62 and 2.50 μm respectively for a mass of 120 g. The closeness of the curves after 210 g reveals a lesser effect of the chemical treatment on the erosion resistance beyond a certain point.

The roughness curves show a typical behaviour encountered in brittle materials wear damage in function of time. From the roughness values, it is evident that chemically strengthened samples present the highest resistance to erosion. This can be explained by the increased fracture toughness due to the treatment.

### 3.4. Optical transmission

The transmission measurements were carried out at 550 nm. Fig. 11 shows the average values of the optical transmission before and after sand blasting with a mass of 210 g at a velocity of 12 m/s normally projected on the samples. The optical transmission drops sharply from a value of 91.5% for the as received glass before erosion tests towards 8.5, 9.9 and 12.9% after erosion respectively for the as received, annealed and toughened glass states. Here also, the chemical treatment does not improve much this optical property.

The micrographs A, B and C shown in Fig. 12 correspond to the damaged zones after a sand blasting with a cumulative erodent mass of 210 g for respectively the as received, the annealed and the chemically treated glass states. We observe that the damaged zones become translucent with a slight difference discernible through the contrasts between the eroded and noneroded zones for the three cases. This contrast diminishes gradually for the three state in the following order: as received (A), annealed (B) and strengthened state (C). The hazeness measured with a Hazemeter XL-211 is about 96, 90

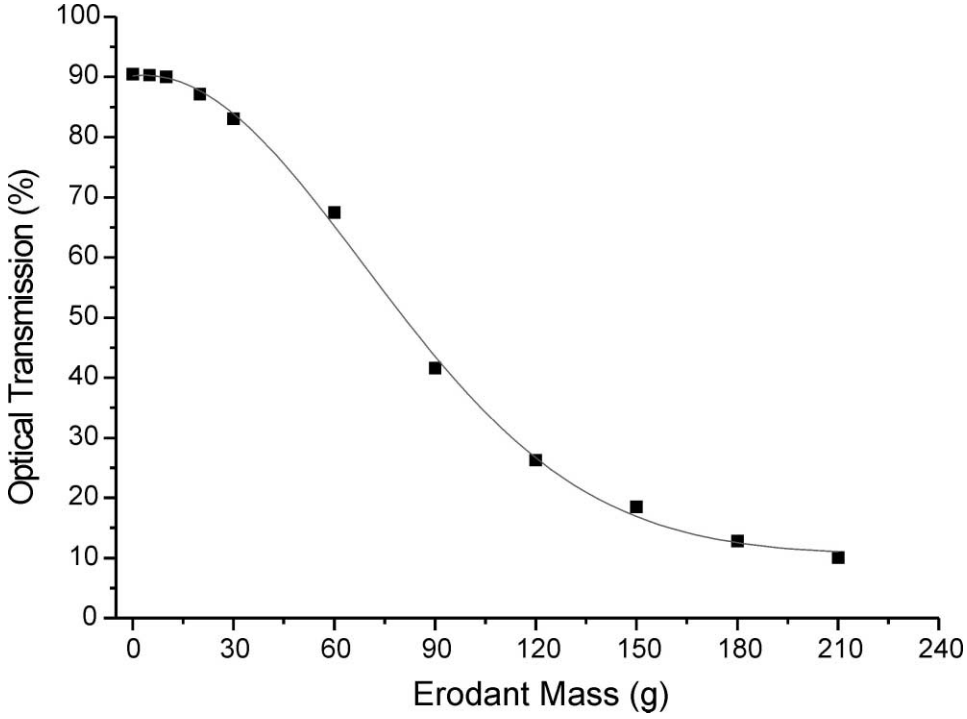


Fig. 13. Optical transmission evolution with cumulative erodant mass for annealed glass state.

and 85% respectively for as received, annealed and chemically treated states.

An example of the optical transmission evolution with cumulative eroding mass for the annealed state shown in Fig. 13 reveals a Gaussian form.

## 4. Conclusion

In order to study the effect of ion exchange strengthening on the erosion wear resistance of a soda lime glass, we proceeded to successive incremental erosion tests using small masses up to 210 g on glass samples in their as received state and when strengthened by ion exchange at normal incidence with a velocity of 12 m/s. A part of the experiment as received glass samples were submitted to an annealing treatment after each incremental test in order to examine the effect of the residual stresses introduced during sand blasting. The sand used presents a varied mineralogical composition. It was used in its rough state. Most particles are rounded in shape and have a size within the interval (200–250) μm. Their average microhardness is $14.49 \pm 3.28$ GPa for an indentation load of 0.6 N.

The evolution of the mass loss and the erosion rate as a function of the eroding mass used incrementally on the different sets of glass samples shows that the ion exchange strengthening provides a limited improvement of the glass erosion resistance. The fact that this treatment is only effective for small masses can be explained by the shallowness of the glass layer submitted to ion exchange and its improved mechanical properties. The measured micro hardness and fracture toughness of the strengthened glass ($Hv = 6.61$ GPa, $K_{IC} = 1.85$ MPa$\sqrt{m}$) are higher than those of as received glass ($Hv = 5.78$ GPa, $K_{IC} = 0.84$ MPa$\sqrt{m}$). All the mean arithmetic roughness curves show a maximum in the interval (90–120) grams and tend after a slight decrease toward the same value ($Ra \approx 2.2$ μm). Besides the problem of the shallow thickness of the compressive layer obtained, a rapid optical degradation was also observed. The optical transmission of the strengthened glass dropped from 91.5 to 12.9% after sand blasting with a mass of 210 g. The damaged zone becomes translucent. The annealing treatment made after each incremental erosion test revealed that the residual stresses introduced during sand blasting enhance somehow the mass loss.

## Acknowledgements

The authors are grateful to Dr. S. Roux (Laboratoire Mixte CNRS- Saint Gobain Recherche, Paris) for his useful suggestions and Mrs G. Duisit (Saint Gobain Recherche, Paris) for sand mineralogical analysis and Mohs's hardness measurements.

## References

1. Hutchings, I. M., *Tribology: Friction and Wear of Engineering Materials*. Metallurgy & Material Science Series, 1992.
2. Wiederhorn, S. M. and Hockey, B. J., Effect of material parameters on the erosion resistance of brittle materials. *J. Mater. Sci.*, 1983, **18**, 766–780.
3. Ritter, J. E. *et al.*, Erosion damage in glass and alumina. *J. Am. Ceram. Soc.*, 1984, **67**(11), 769–774.
4. Buijs, M., Erosion of glass as modeled by indentation theory. *J. Am. Ceram. Soc.*, 1994, **77**(6), 1676–1678.
5. Evans, A. G., Gulden, M. E. and Hockey, B. J., Effect of material parameters on the erosion of brittle materials in the elastic-plastic response regime. *Proc. Res. Soc. London, Ser. A*, 1978, **361**, 343–365.
6. Wada, S. and Watanabe, N., Solid particle erosion of brittle materials—part 4: the erosive wear of thirteen kinds of commercial $Al_2O_3$ ceramics. *Yogyo-Kyokai. Shi*, 1987, **95**(9), 835–840.
7. Wada, S. and Watanabe, N., Solid particle erosion of brittle materials—part 2: the relation between erosive wear and α- or β-phase content of hot pressed $Si_3N_4$. *Yogyo-Kyokai. Shi*, 1987, **95**(5), 468–471.
8. Wada, S., Watanabe, N. and Tani, T., Solid particle erosion of brittle materials—part 6: the erosive wear of $Al_2O_3$–SiC composites. *Yogyo-Kyokai. Shi*, 1988, **96**(2), 111–118.
9. Lawn, B. R. and Marshall, D. B., Hardness, toughness and brittleness: an indentation analysis. *J. Am. Ceram. Soc.*, 1979, **62**(7–8), 347–350.
10. Sargent, G.A., Mehrotra, P.K., Conrad, H., Proceedings of the 5th International Conference on Erosion by Solid and Liquid Impact. Cambridge, England, August 1979, 1979, Cambrigde University Press, Cambridge.
11. Mehrotra, P. K., Sargent, G. A. and Conrad, H., A computer simulation of the time dependence of the erosion of pyrex glass by glass beads. *J. Mater. Sci.*, 1982, **17**, 1049–1058.
12. Lawn, B. R. and Wilshaw, R., Review paper on indentation fracture: principles and applications. *J. Mater. Sci.*, 1975, **10**, 1049–1081.
13. Shipway, P. H. and Hutchings, I. M., The role of particle properties in the erosion of brittle materials. *Wear*, 1996, **193**, 105–113.
14. Wada, S. and Watanabe, N., Solid particle erosion of brittle materials—part 4: the interaction with material properties of target and that of impingement particle on erosive wear mechanisms. *Yogyo-Kyokai. Shi*, 1987, **95**(6), 573–578.
15. Wada, S., Effect of the fracture toughness of impact particle on the erosive wear of ceramics. *J. Jap. Soc. Powder Powder Metall.*, 1991, **38**, 893–894.
16. Bousid, S. and Bouaouadja, N., Effects of impact angles on glass surface eroded by sand blasting. *J. Eur. Cer. Soc.*, 2000, **20**(4), 481–488.
17. Sheldom, G. L., *Trans. ASME B, J. Eng. Industry*, 1966, **88**, 387–392.
18. Manish, R., Vishwanathan, B. and Sundarajan, G., The solid particle of polymer matrix composites. *Wear*, 1994, **171**, 149–161.
19. Hutchings, I. M., Transition, threshold effect and erosion maps. *Key Eng. Mater.*, 1992, **71**, 298–311.
20. Verspui, M. A. *et al.*, Validation of the erosion map for spherical particle impacts on glass. *Wear*, 1998, **215**, 77–82.
21. Banerjee, R. and Sarkat, B. K., Indentation fatigue of soda-lime-silica glass. *Glastech. Ber. Glass Sci.*, 1995, **68**(6), 177–180.
22. Watson, H., *Glasses and Their Applications*. The Institute of Metals, 1991.
23. Lawn, B. R., Marshall, D. B. and Wiederhorn, S. M., Strength degradation of glass impacted with sharp particles: II, Tempered glass. *J. Am. Ceram. Soc.*, 1979, **62**(2–3), 71–74.
24. Tandon, R. and Cook, R. E., Indentation crack initiation and propagation in tempered glass. *J. Am. Ceram. Soc.*, 1993, **76**(4), 885–889.

25. Hara, M. and Kerkhof, F., Vickers hardness of toughened sheet glass. *Rep. Res. Lab. Asahi Glass,* 1962, **12**(2), 99–104 (in Japanese with English Abstract).
26. Hara, M., Some aspects of strength characteristics of glass. *Glasstech. Ber. Glass Sci.*, 1988, **61**(7), 191–196.
27. Donald, I. W. *et al.*, The mechanical properties and fracture behavior of some chemically strenghtened silicate and borate glasses. *Glass Techn.*, 1993, **34**(3), 114–119.
28. Donald, I. W., Review: methods for improving the mechanical properties of oxide glasses. *J. Mater. Sci.*, 1989, **24**, 4177–4208.
29. Gy, R., L'endommagement mécanique de la surface du verre. *Verre*, 1997, **3**(3), 21–28.
30. Tandon, R. and Green, D. J., Indentation behaviour of ion-exchanged glasses. *J. Am. Ceram. Soc.*, 1990, **73**(4), 970–977.
31. Cho, S. J., Jeon, S. B., Kim, J. J. and Moon, H., Enhancement of sliding wear resistance of glass ion-exchange. *J. Mater. Sci. Letters*, 1990, **19**, 596–597.
32. Hajji, P. *et al.*, Amélioration de la résistance mécanique des verres par revêtements à base de polymères. *Verre*, 2000, **6**(2), 9–21.
33. Niihara, K. et al., In *Indentation Fracture Toughness of Brittle Materials for Palmqvist Cracks, Fracture Mechanics of Ceramics, Vol. 5*, ed. R. C. Bradt, A.G., Evans, P.P. Hasselman, P.P. and F. F. Lange. Plenum Press, New York, 1983, pp. 97–105.
34. DIN 50332, *Strahlverschleiβprufung*. DIN, Berlin, 1984.
35. ASTM G76–89, *Standard Practice for Conducting Erosion Tests by Solid Particle Impingement Using Gas Jets*. ASTM, Philadelphia, 1992.
36. Sheldon, G. L. *et al.*, Erosion of a tube by gas-particle flow. Trans. ASME. *J. Eng. Mater. Technol.*, 1977, **99**, 138–142.
37. Hutchings, I. M., *Tribology*. Edward Arnold, 1992.
38. Shipway, P. H. *et al.*, Influence of nozzle roughness on condition in a gas-blast erosion rig of sand blasting. *Wear*, 1993, **162/164**, 148–158.
39. Chevalier, P., Vannes, A.B., Effects on a sheet surface of an erosive particle jet upon impact, *Wear*, **184**, 1994, 87–91.
40. Haugen, K. *et al.*, Sand erosion of wear-resistant material: erosion in shock valves. *Wear*, 1995, **186/187**, 179–188.
41. Slikkerveer, P. J. *et al.*, Erosion and damage by sharp particles. *Wear*, 1998, **217**, 237–250.
42. Wood, R. J. K., Design and performance of a high velocity air–sand jet impingement erosion facility. *Wear*, 1998, **220**, 95–112.
43. Thiruvengadaswamy, R. and Scattergood, R. O., Indentation cycling tests on soda lime glass. *J. Am. Ceram. Soc.*, 1993, **76**(6), 1611–1614.